Metallurgy and Foundry Engineering – Vol. 40, 2014, No. 1, pp. 45–54
http://dx.doi.org/10.7494/mafe.2014.40.1.45

**Krzysztof Ziewiec, Krystian Prusik, Mirosława Różycka**

# Amorphization and liquid state separation in $Ni_{80-2x}Cu_xFe_xP_{20}$ alloys

## Amorfizacja i podział w stanie ciekłym w stopach $Ni_{80-2x}Cu_xFe_xP_{20}$

**Abstract**

The aim of the work is to study the ability and potential of glass formation in Ni-Fe-Cu-P alloys. A series of alloys were produced in arc furnace (i.e. $Ni_{70}Fe_5Cu_5P_{20}$, $Ni_{60}Fe_{10}Cu_{10}P_{20}$, $Ni_{50}Fe_{15}Cu_{15}P_{20}$, $Ni_{40}Fe_{20}Cu_{20}P_{20}$, $Ni_{30}Fe_{25}Cu_{25}P_{20}$, $Ni_{20}Fe_{30}Cu_{30}P_{20}$). The primary microstructure of the ingots was studied. The ribbons in as-melt-spun state were characterized by X-ray diffraction (XRD). The $Ni_{70}Fe_5Cu_5P_{20}$, $Ni_{60}Fe_{10}Cu_{10}P_{20}$ melt-spun alloys were found to be amorphous. For higher copper and iron concentrations a crystalline structure was obtained after melt spinning. This correlated with the tendency for the formation of the Fe-based phases enriched in P and Cu-based poorly alloyed phases which resulted in the formation of crystalline microstructure in melt-spun ribbons. For higher concentration of Fe and Cu, microstructures of the alloys contained constituents resultant from a tendency for separation in the liquid state. It is observed that the formation of the crystalline melt-spun ribbons is caused by the attraction of phosphorus by iron and the formation of copper-based fcc phase.

**Key words:** amorphous materials, amorphization, X-ray diffraction, transmission electron microscopy

**Streszczenie**

Celem pracy było zbadanie podatności na zeszklenie oraz możliwości wytworzenia struktury szklistej w stopach wieloskładnikowych Ni-Fe-Cu-P. W piecu łukowym wytworzono serię stopów (tzn.: $Ni_{70}Fe_5Cu_5P_{20}$, $Ni_{60}Fe_{10}Cu_{10}P_{20}$, $Ni_{50}Fe_{15}Cu_{15}P_{20}$, $Ni_{40}Fe_{20}Cu_{20}P_{20}$, $Ni_{30}Fe_{25}Cu_{25}P_{20}$, $Ni_{20}Fe_{30}Cu_{30}P_{20}$). Badano strukturę pierwotną wlewków. Taśmy w stanie po odlewaniu na wirujący bęben badano za pomocą dyfrakcji rentgenowskiej.

**Krzysztof Ziewiec Associate Professor, Ph.D., Eng.:** Institute of Technology, Faculty of Mathematics, Physics and Technical Science, Pedagogical University of Cracow, kziewiec@up.krakow.pl; **Krystian Prusik Ph.D.:** Faculty of Computer Science and Materials Science, University of Silesia, Chorzów; **Mirosława Różycka M.Sc. Eng.:** AGH University of Science and Technology, Faculty of Metals Engineering and Industrial Computer Science, Krakow, Poland

Stwierdzono, że stopy $Ni_{70}Fe_5Cu_5P_{20}$, $Ni_{60}Fe_{10}Cu_{10}P_{20}$ odlewane na wirujący bęben były amorficzne. Dla stopów o wyższych zawartościach miedzi i żelaza po odlewaniu na wirujący walec otrzymano strukturę krystaliczną. Fakt ten można powiązać z tendencją do tworzenia faz na osnowie żelaza wzbogaconych w fosfor oraz zubożonych w pozostałe składniki stopowe faz na osnowie miedzi, które przyczyniły się do tworzenia w odlewanych taśmach mikrostruktury krystalicznej. Dla wyższych zawartości żelaza i miedzi, mikrostruktury stopów zawierały składniki fazowe powstające w efekcie tendencji stopów do podziału fazowego w stanie ciekłym. Zaobserwowano, że tworzenie krystalicznych taśm jest spowodowane przez przyciąganie fosforu przez żelazo oraz tworzenie bogatej w miedź fazy o strukturze regularnej ściennie centrowanej.

**Słowa kluczowe:** materiały amorficzne, amorfizacja, dyfrakcja rentgenowska, transmisyjna mikroskopia elektronowa

## 1. Introduction

The unique properties of the amorphous alloys [1–3] are very vital for practical applications in many structural and functional materials. It is also well known that liquid immiscibility can negatively influence the glass forming ability. However, there are applications where it is useful to produce a composite material that combines the properties of the amorphous matrix and a highly dispersed fine crystalline phase [4]. This is potentially useful in improving ductility using a soft crystalline phase or increasing coercivity in hard magnet structures with the use of a paramagnetic phase. Such efforts have been already done with the aim of improving the ductility by ductile crystalline phase formed in situ [5, 6]. Such composites can be made by introducing the particles ex situ prior to casting [5–7], or by the formation of the crystalline phase in situ. The latter can be carried out by the crystallization of the amorphous matrix or the formation of the crystalline phase during casting [8–13]. It is also possible to use liquid immiscible alloys for this purpose [12–14].

Therefore, the exploration of the alloys and systems with glass forming potential and liquid immiscibility is potentially interesting in terms of providing amorphous matrix alloys with the ability to control their microstructure. The Ni-Fe-Cu-P system provides the glass forming alloys [15–19], on the other hand a relatively high positive enthalpy of mixing between Fe and Cu [20] justify the expectation that for some compositions liquid miscibility gap can be observed in the Ni-Fe-Cu-P system. The aim of the work is to investigate the range of the glass forming compositions in a series of alloys $Ni_{80-2x}Cu_xFe_xP_{20}$, where $x = 5$, 10, 15, 20, 25 and 30.

## 2. Experimental

A series of alloys $Ni_{80-2x}Cu_xFe_xP_{20}$, where $x = 5$, 10, 15, 20, 25 and 30 were prepared using 99.95 wt % Ni, 99.95 wt % Cu, 99.95 wt % Fe, Ni-P, Cu-P and Fe-P master alloys The alloys

were made from precursors that were melted under argon in the arc furnace. Then, the alloys were induction melted in quartz tubes under a vacuum ($10^{-2}$ bar) and quenched in water to obtain an ingot of 10 mm in diameter. The primary microstructure of the ingots was studied under a light microscope using OLYMPUS GX51. Then, the alloys were melt-spun at with linear speed of 33 m/s. The argon was used as protective atmosphere and the ejection overpressure was 150 kPa. The selected alloys were investigated by means of the JEOL 300kV transmission electron microscope (TEM) and X-ray diffractions (XRD) of the alloys were performed using DRON-3 powder diffractometer using $CuK_{\alpha}$ radiation. The scattering angle $2\Theta$ was varied with the constant step of 0.02 degree. Scans were performed in the $\Theta - 2\Theta$ mode.

## 3. Results and discussion

The microstructure of the induction melted ingots are presented in Figure 1. The microphotographs of the alloys $Ni_{70}Cu_5Fe_5P_{20}$ (Fig. 1a) and $Ni_{60}Cu_{10}Fe_{10}P_{20}$ (Fig. 1b) show that during the crystallization in the quartz tubes immersed in water the eutectic microstructure is formed. As the average concentrations of copper and iron are increased in $Ni_{50}Fe_{15}Cu_{15}P_{20}$ (Fig. 1c), the reduction of the eutectic at the cost of the primary dendrites is observed. The microstructure is slightly hypo-eutectic. In the $Ni_{40}Cu_{20}Fe_{20}P_{20}$ (Fig. 1d) there are more dendrites. The dendrites contain probably less phosphorus and correspond to a Fe-Ni-rich solid solution and the constituent represented by the bright regions has morphology often met in phosphide constituents.

In the latter alloy the fine eutectic constituent is a minor one. Further increase of copper and iron content in the ingot of the $Ni_{30}Fe_{25}Cu_{25}P_{20}$ alloy (Fig. 1e) results in the microstructure composed only of dendrites and phosphide regions. The fine eutectic is not present in the microstructure of this alloy. However, for the sample with the highest content of copper and iron i.e. $Ni_{20}Fe_{30}Cu_{30}P_{20}$ (Fig. 1f) shows definitely a different microstructure than the one observed in the alloys containing less copper and iron. The darker regions represent Cu-rich solid solution and the brighter intergranular regions are composed of the dark and bright constituents. The latter regions are obviously enriched in Fe, Ni and P. The most important feature of the alloy is that the morphology of the microstructural constituents is typical for the liquid immiscible alloys. Probably the two main microstructural constituents of the alloy separated already in the liquid state.

The TEM micrograph of the melt spun $Ni_{60}Cu_{10}Fe_{10}P_{20}$ alloy is presented in Figure 2. The microstructure of the alloy is representative for the alloys with low content of Cu and Fe up to $x = 10$ and it is amorphous, which is confirmed by the broad diffusive rings of the electron diffraction pattern (Fig. 2). However, for the higher values of x samples were not amorphous. An exemplary TEM microstructures for these crystalline alloys are presented in Figure 3 and Figure 4.

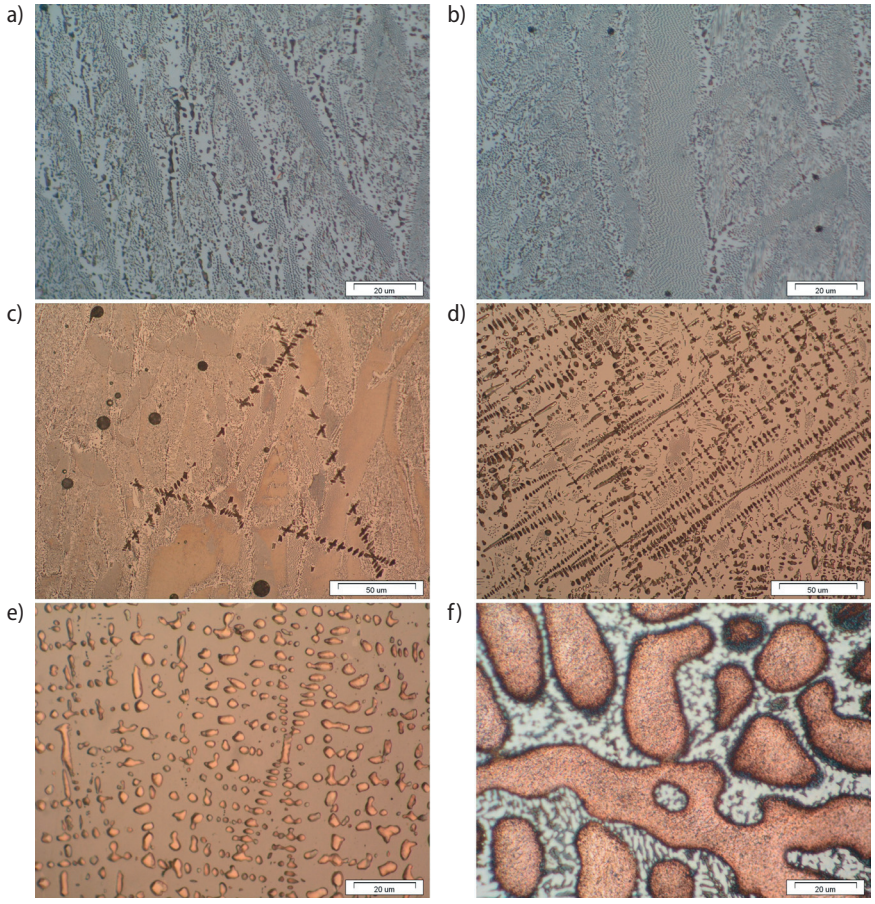


*Fig. 1. Primary microstructure of ingots solidified in quartz tubes quenched in water: (a) $Ni_{70}Cu_5Fe_5P_{20}$; (b) $Ni_{60}Cu_{10}Fe_{10}P_{20}$; (c) $Ni_{50}Fe_{15}Cu_{15}P_{20}$; (d) $Ni_{40}Cu_{20}Fe_{20}P_{20}$; (e) $Ni_{30}Fe_{25}Cu_{25}P_{20}$, (f) $Ni_{20}Fe_{30}Cu_{30}P_{20}$*

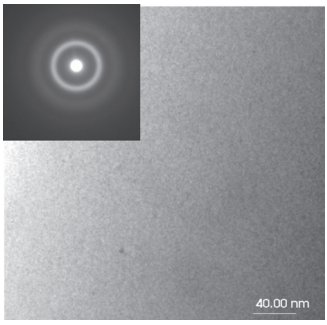


*Fig. 2. TEM microstructure and electron diffraction pattern obtained from the $Ni_{60}Cu_{10}Fe_{10}P_{20}$ melt-spun ribbon*

During the melt spinning, the immiscible $Ni_{20}Cu_{30}Fe_{30}P_{20}$ formed the two products instead of a single-component ribbon. One of them were gray plates and the other golden needles. The TEM microstructure of the gray plates is presented in Figure 3 and the one for the golden needles is in Figure 4. The gray plates formed from the $Ni_{20}Cu_{30}Fe_{30}P_{20}$ alloy during the melt spinning present fine crystalline microstructure with the grain size in a range from tens of nanometers to hundreds of nanometers (Fig. 3a). The electron diffraction pattern obtained from the extensive area presents a series of rings that can be attributed to the fine crystallites of the three phases (Fig. 3b, c, d). The first is very close to face centered cubic Cu-Ni solid solution (space group 225 (Fm-3m), lattice parameter a = 3.610Å) (Fig. 3b). The second phase is $M_3P$ type phosphide isomorphic with tetragonal $Fe_{1.33}Ni_{1.67}P$ (space group 82 (I-4)), lattice parameters a = 9.044Å, b = 4.464Å (Fig. 3c). The third phase is $M_2P$ type phosphide isomorphic with hexagonal $Fe_2P$ (space group 189 (P-62m), lattice parameters a = 5.867Å, b = 5.867Å, c = 4.464Å (Fig. 3d). The TEM microstructure of the golden needles formed from the $Ni_{20}Cu_{30}Fe_{30}P_{20}$ alloy during the melt spinning shown on Figure 4a consists of globular precipitates within the matrix. The HRTEM micrograph from such the precipitate is presented in Figure 4b. Figure 4c shows the Fourier transform (FT) image and its solution which can be attributed to the $[\bar{2}11]$ zone axis of the hexagonal $M_2P$ phosphide. Electron diffraction from the matrix is presented in Figure 4d. The pattern can be assigned to the $[\bar{1}0\bar{1}]$ zone axis of the Cu-based fcc solid solution.

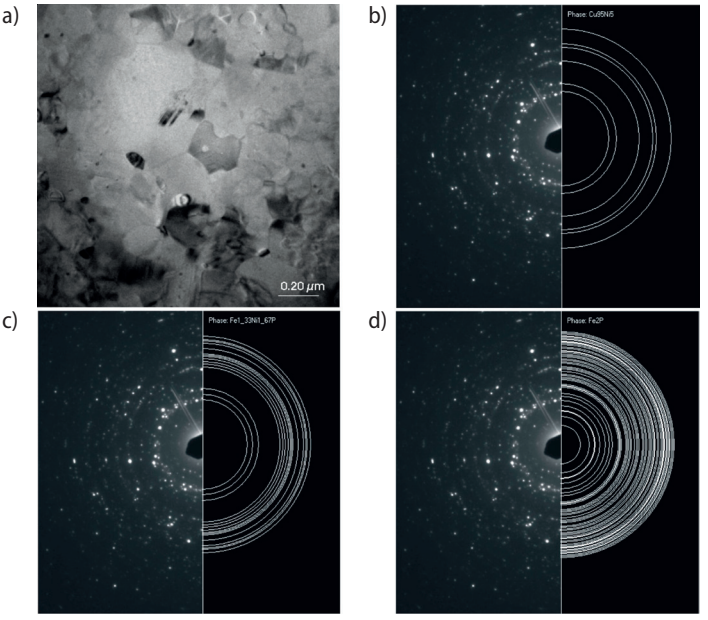


*Fig. 3. TEM microstructure (a) and electron diffraction pattern obtained from the gray plates of the $Ni_{20}Cu_{30}Fe_{30}P_{20}$ melt-spun alloy. The matched ring patters may be identified as: (b) $Cu_{95}Ni_5$ fcc solid solution; (c) $M_3P$ type phosphide isomorphic with tetragonal $Fe_{1.33}Ni_{1.67}P$ (I-4); (d) $M_2P$ type phosphide isomorphic with hexagonal $Fe_2P$ (P-62m)*

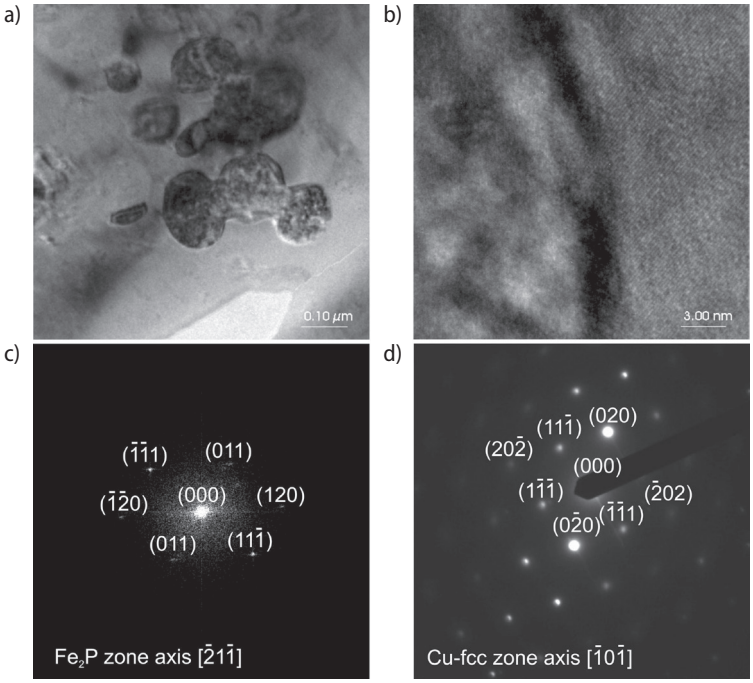


*Fig. 4. TEM microstructure (a) and HRTEM image obtained from the golden needles of the $Ni_{20}Cu_{30}Fe_{30}P_{20}$ melt-spun alloy (b); (c) FFT of the HRTEM from (b) matched as the image of the $[2\bar{1}\bar{1}]$ zone axis of the hexagonal $M_2P$ phosphide: (d) diffraction from the matrix identified as $[\bar{1}0\bar{1}]$ zone axis of the Cu-based fcc solid solution*

The X-ray diffraction patterns obtained for the alloys $Ni_{70}Cu_5Fe_5P_{20}$, $Ni_{60}Cu_{10}Fe_{10}P_{20}$, $Ni_{40}Cu_{20}Fe_{20}P_{20}$ and $Ni_{20}Cu_{30}Fe_{30}P_{20}$ melt spun alloys are presented in Figure 5. The latter alloy separated during chilling on a copper roller, thus the two XRD were registered – one for the golden needles and one for the grey plates. The XRD for $Ni_{70}Cu_5Fe_5P_{20}$ and $Ni_{60}Cu_{10}Fe_{10}P_{20}$ melt spun ribbons has of a broad diffraction maximum located between 40°–50° (2Θ) which can be attributed to their amorphous state. However, $Ni_{40}Cu_{20}Fe_{20}P_{20}$ was not amorphous and the peaks from crystalline phases can be identified on the diffraction. One phase is fcc Cu-Ni solid solution and the second phase is $M_3P$ type phosphide isomorphic with tetragonal $Fe_{1.33}Ni_{1.67}P$. Regarding the two products obtained for the $Ni_{20}Cu_{30}Fe_{30}P_{20}$ alloy the peaks can be attributed to the three phases. Similarly, as in the TEM study they were fcc Cu-Ni solid solution and the second phase is $M_3P$ type phosphide isomorphic with tetragonal $Fe_{1.33}Ni_{1.67}P$ and $M_2P$ type phosphide, respectively. However, the relative intensities of the three phases were distinctly different in the two separated products. Generally, lower intensities and broader peaks can be observed for the golden needles than for the grey plates. This may suggest the finer crystalline structure of the former product.

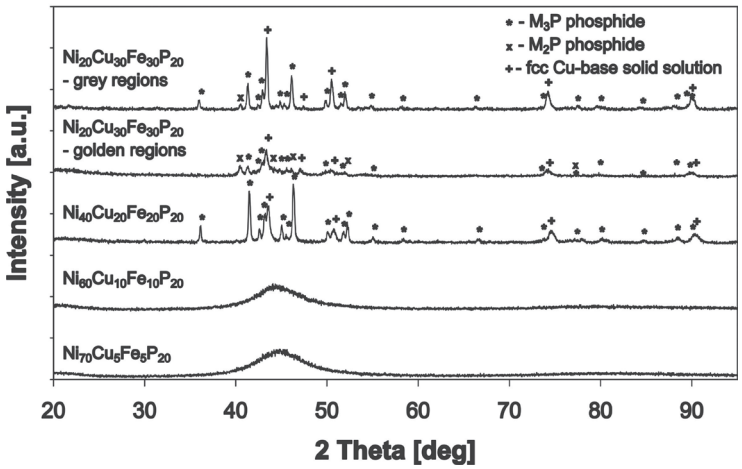


*Fig. 5. X-ray diffraction patterns of the $Ni_{70}Cu_5Fe_5P_{20}$, $Ni_{60}Cu_{10}Fe_{10}P_{20}$, $Ni_{40}Cu_{20}Fe_{20}$ and the two products of the $Ni_{20}Cu_{30}Fe_{30}P_{20}$ melt-spun alloy i.e. golden needles and gray plates*

The results of the investigations can be interpreted in terms of mutual affinity and tendency for attraction or repulsion of the particular pairs of chemical elements. The Table 1 presents heats of mixing for liquid binary alloys $\Delta H^{mix}$ [20, 21].

*Table 1. Heats of mixing for liquid binary alloys $\Delta H^{mix}$ [kJ/mole] [20, 21]*

| Element | Ni | Fe | Cu | P |
|---|---|---|---|---|
| Ni | 0 | -2 | +4 | 26 |
| Fe | | 0 | +13 | –31 |
| Cu | | | 0 | –17.5 |
| P | | | | 0 |

It is well known that the relatively high enthalpies of mixing between the elemental constituents of the alloy correlate well with its good glass forming ability. For Ni-Cu-Fe-P system all of the metallic elements fulfill the condition with relation to P. It is also well known that there are a number of both Ni-based and Cu-based amorphous alloys with phosphorus [22–25]. However, in the present work it is shown that a sufficiently high content of Ni in the alloy and relatively low Fe and Cu content cause that the latter two elements are diluted enough in Ni-P liquid and there is no partitioning in the liquid state in spite of the relatively high positive enthalpy of mixing between Fe and Cu.

However, for a sufficiently low concentration of the Ni in the alloy and high content of the Fe and Cu, the tendency for the formation of iron and nickel phosphides and

impoverishing of the Cu-based liquid is predominating which finally leads to a lack of glass forming ability in spite of the fact that the composition assures relatively high enthalpies of mixing between the elemental constituents.

The separation of the liquid on Fe-rich and Cu-rich liquids during the solidification of the ingot in the $Ni_{20}Cu_{30}Fe_{30}P_{20}$ alloy and formation of the two separated products (the gray plates and the golden needles) during the melt spinning process of the alloy correlates well with observation that the abundance of Fe and Cu and their relatively high enthalpy of mixing leads to the attraction of Fe and P and at the same time causes formation of low alloyed Cu-based liquid. Low content of Ni in the alloy does not assure formation of the uniform liquid that can be stable enough to form metallic glass below the glass transition temperature, because both liquids Fe-rich and Cu-rich are below their $T_0$ temperatures [26]. It is worth to note that there are Fe-based alloys where in spite of a substantial concentration of Cu the vitrification of the matrix was obtained [27–34].

## 4. Summary

The $Ni_{80-2x}Cu_xFe_xP_{20}$ alloys show the formation of differentiated microstructures, both during solidification of ingots in quartz tubes and melt spinning. This depends on the contents of Fe and Cu that have a relatively high positive enthalpy of mixing to each other. For ingots, the increase of copper and iron had gradually eliminated the eutectic constituent and finally led to microstructure where separation in the liquid state was evident. For rapidly cooled melt spun ribbons, the increase of Fe and Cu caused the transition from fully amorphous structures to crystalline. The highest Fe and Cu concentrations also caused partitioning in the liquid state, resulting in the formation of the two products of the liquid separation even in conditions of rapid cooling provided by the melt spinning technique. For the highest concentrations of Fe and Cu the low content of Ni in the alloy does not assure the formation of the uniform liquid that can be stable enough to form metallic glass below the glass transition temperature, because both liquids Fe-rich and Cu-rich are below their $T_0$ temperatures, thus are unable to form an amorphous structure.

### Acknowledgements

Project co-financed by the European Regional Development Fund under the Infrastructure and Environment Programme.

### References

[1] Yoshizawa Y., Oguma W., Yamauchi K.: *New Fe-based soft magnetic alloys composed of ultrafine grain-structure*. Journal of Applied Physics, 64 (1988), 6044–6046

[2] Shen T.D., Schwarz R.B.: *Bulk ferromagnetic glasses in the Fe–Ni–P–B system*. Acta Materialia, 49 (2001), 837–847

[3] Conner R.D., Rosakis A.J., Johnson W.L., Owen D.M.: *Fracture toughness determination for a beryllium-bearing bulk metallic glass*. Scripta Materialia, 37 (1997), 1373–1378
[4] Peker A., Johnson W.L.: *A highly processable metallic glass: $Zr_{41.2}Ti_{13.8}Cu_{12.5}Ni_{10.0}Be_{22.5}$*. Applied Physics Letters, 63 (1993), 2342–2344
[5] He Y., Schwarz R.B., Archuleta J.I.: *Bulk glass formation in the Pd–Ni–P system*. Applied Physics Letters, 69 (1996), 1861–1863
[6] Ziewiec K., Bryła K., Ziewiec A., Prusik K.: *The microstructure and properties of a new $Fe_{41}Ni_{39}P_{10}Si_5B_5$ glass forming alloy*. Archives of Materials Science and Engineering, 34 (2008), 35–38
[7] Lee S.-W., Huh M.-Y., Fleury E., Lee J.-C.: *Crystallization-induced plasticity of Cu–Zr containing bulk amorphous alloys*. Acta Materialia, 54 (2006), 349–355
[8] Szuecs F., Kim C.P., Johnson W.L.: *Mechanical properties of $Zr_{56.2}Ti_{13.8}Nb_{5.0}Cu_{6.9}Ni_{5.6}Be_{12.5}$ ductile phase reinforced bulk metallic glass composite*. Acta Materialia, 49 (2001), 1507–1513
[9] Choi-Yim H., Conner R.D., Johnson W.L.: *Processing, microstructure and properties of bulk metallic glass composites*. Annales de Chimie – Science des Matériaux, 27, 5 (2002), 113–118
[10] Tan H., Zhang Y., Li Y.: *Synthesis of La-based in-situ bulk metallic glass matrix composite*. Intermetallics, 10 (2002), 1203–1205
[11] Wang Q., Balandin J.-J., *Suery M., Van de Moortele B., Pelletier J.-M.: High temperature deformation of a fully amorphous and partially crystallized bulk metallic glass*. Annales de Chimie – Science des Materiaux, 27, 5 (2002), 19–24
[12] Hu X., Ng S.C., Feng Y.P., Li Y.: *Glass forming ability and in-situ composite formation in Pd-based bulk metallic glasses*. Acta Materialia, 51 (2003), 561–572
[13] Eckert J., Kühn U., Mattern N., He G., Gebert A.: *Structural bulk metallic glasses with different length-scale of constituent phases*. Intermetallics, 10 (2002), 1183–1190
[14] Ziewiec K.: *Characterization of immiscible Ni78Ag2P20 alloy and formation of amorphous/crystalline composite*. Journal of Non-Crystalline Solids, 355 (2009), 2540–2543
[15] Ziewiec K., Malczewski P., Boczkal G., Prusik K.: *Formation and properties of amorphous/crystalline ductile composites in Ni-Ag-P immiscible alloys*. Solid State Phenomena, 186 (2012), 216–221
[16] Kozieł T., Kędzierski Z., Zielińska-Lipiec A., Latuch J.: *The microstructure of melt-spun alloys with liquid miscibility gap*. Journal of Physics: Conference Series 144, 2009, 012093-1–012093-4
[17] Ziewiec K., Olszewski P., Gajerski R., Kąc S., Ziewiec A., Kędzierski Z.: *Glass forming ability and thermal stability of $Ni_{63}Cu_9Fe_8P_{20}$ melt spun ribbon*. Journal of Non-Crystalline Solids, 343 (2004), 150–153
[18] Ziewiec K., Lelątko J., Pączkowski P., Bryła K.: *Devitrification and Nano-Crystalline/Amorphous Composite Formation in $Ni_{64}Cu_9Fe_8P_{19}$ Glassy Alloy at Elevated Temperatures*. Solid State Phenomena, 130 (2007), 167–170
[19] Ziewiec K., Bryła K., Błachowski A., Ruebenbauer K., Przewoźnik J.: *Characterisation and structure development of $Ni_{64}Cu_9Fe_8P_{19}$ glass forming alloy at elevated temperatures*. Journal of Alloys and Compounds, 429 (2007), 133–139
[20] Boer F.R., Boom R., Mattens W.C.M., Miedema A.R., Niessen A.K.: *Cohesion and structure, Cohesion in metals*. Vol. 1. Elsevier Science, Amsterdam, 1988
[21] Griesche A., Macht M.-P., Frohberg G.: *Chemical diffusion in bulk glass-forming $Pd_{40}Cu_{30}Ni_{10}P_{20}$ melts*. Scripta Materialia, 53 (2005), 1395–1400
[22] Ziewiec K., Kędzierski Z., Dargel-Sulir L., Gajerski R.: *X-ray studies of $Ni_{78}P_{13}$ and $Ni_{81}P_{19}$ electroless alloys in as-deposited and heat treated state*. Metallurgy of Foundry and Engineering, 26, 2 (2000), 121–126
[23] Ziewiec K., Kędzierski Z., Morgiel J.: *Kinetics of phase transformations in Ni-P alloys upon heating.* Metallurgy and Foundry Engineering, 28, 2 (2002), 157–166

[24] Ziewiec K., Gajerski R., Dutkiewicz J., Król J.: *Thermal behaviour of rapidly quenched Cu-Ni-based alloys with phosphorus*. Metallurgy and Foundry Engineering, 28, 2 (2002), 149–156

[25] Ziewiec K., Olszewski P., Gajerski R., Małecki A.: *Glass forming ability and thermal stability of $Cu_{68.5}Ni_{12}P_{19.5}$ and $Cu_{66}Ni_{11.5}P_{22.5}$ melt spun ribbons*. Journal of Alloys and Compounds, 373 (2004), 115–121

[26] John D.H. St.: *Freezing Diagrams: Part I. Freezing Diagrams: Part I. Development and Implications for Glas Formability*. Metallurgical Transactions, 20A (1989), 289–297

[27] Ziewiec K., Kędzierski Z.: *The microstructure development in $Fe_{32}Cu_{20}Ni_{28}P_{10}Si_5B_5$ immiscible alloy and possibilities of formation of amorphous/crystalline composite*. Journal of Alloys Compounds, 480 (2009), 306–310

[28] Ziewiec K., Ziewiec A., Prusik K.: *Microstructures in $Fe_{30}Ni_{30}Cu_{20}P_{10}Si_5B_5$ melt-spun alloy ejected at various temperatures.* Journal of Achievments in Materials and Manufacture Engineering, 37, 2 (2009), 532–537

[29] Ziewiec K., Malczewski P., Gajerski R., Ziewiec A.: *The microstructure development in arc-melt and melt-spun $Fe_{50}Ni_{10}Cu_{20}P_{10}Si_5B_5$ immiscible alloy*. Journal of Non-Crystalline Solids, 357 (2011), 73–77

[30] Ziewiec K., Malczewski P., Prusik K.: *Transformations in liquid state and microstructure analysis in immiscible in $Fe_{60}Cu_{20}P_{10}Si_5B_5$ alloy*. Inżynieria Materiałowa, 1 (2011), 26–29

[31] Kozieł T., Kędzierski Z., Zielińska-Lipiec A., Ziewiec K.: *The microstructure of liquid immiscible Fe–Cu-based in situ formed amorphous/crystalline composite*. Scripta Materialia, 54 (2006), 1991–1995

[32] Kozieł T., Zielińska-Lipiec A., Latuch J., Kąc S.: *Microstructure and properties of the in situ formed amorphous-crystalline composites in the Fe-Cu-based immiscible alloys*, Journal of Alloys and Compounds, 509 (2011), 4891–4895

[33] Kozieł T., Kędzierski Z., Zielińska-Lipiec A., Latuch J., Cieślak G.: *TEM studies of melt-spun alloys with liquid miscibility gap*. Journal of Microscopy, 237, 3 (2010), 267–270

[34] Kozieł T., Zielińska-Lipiec A., Kędzierski Z., Czeppe T.: *Transmission electron microscopy study of crystallization in Fe-Si-B-Cr-C amorphous alloy*. Journal of Microscopy, 224, 1 (2006), 27–29